Cell-Centered Finite Volume Schemes for Semiconductor Device Simulation

Karl Rupp*†, Markus Bina†, Yannick Wimmer*‡, Ansgar Jüngel† and Tibor Grasser*
*Institute for Microelectronics, TU Wien, Austria
†Institute for Analysis and Scientific Computing, TU Wien, Austria
‡Christian Doppler Laboratory for Reliability Issues in Microelectronics at the Institute for Microelectronics
Email: {rupp|bina|wimmer|grasser}@iue.tuwien.ac.at, juengel@asc.tuwien.ac.at

***Abstract*—Although the traditional finite volume scheme based on boxes obtained from the dual Voronoi grid has been employed successfully for classical semiconductor device simulation for decades, certain drawbacks such as the required Delaunay property of the underlying mesh limit its applicability for two- and particularly three-dimensional device simulations on unstructured meshes. We propose a discretization based on *mesh cells* rather than dual boxes around vertices, which circumvents the Delaunay requirement, yet preserves all the important features of the traditional method such as exact current conservation. The applicability of our method is demonstrated for classical and semiclassical models to tackle current engineering problems: We consider three-dimensional drift-diffusion simulations of geometric variations of the fin in a FinFET and present results from spatially two-dimensional simulations of a high-voltage nLDMOS device based on spherical harmonics expansions for direct solutions of the Boltzmann transport equation.**

I. Introduction

The traditional finite volume scheme is the method of choice for semiconductor device simulation. Classical models such as the drift-diffusion or hydrodynamic model associate their unknowns with the vertices of the mesh and use boxes from the dual Voronoi grid as control volumes [1]. For two- and three-dimensional device simulation on unstructured grids, the resolution of complicated geometries results in several problems: First, the dual Voronoi grid only exists for Delaunay meshes, which are challenging to generate especially in three spatial dimensions [2]. This is a serious issue since meshes obtained from a process simulation are usually not Delaunay meshes and have to be converted, which often results in problems. Second, considerable effort is required to deal with vertices connecting two or more different material regions, since the contributions from the two material regions need to be considered correctly, cf. Fig. 1(a).

Alternative discretization schemes have been proposed in the past. One family of methods is derived from classical finite element methods (see for example [3]–[5] and references therein). In order to reflect the desirable property of local charge conservation in the numerical approximation, non-trivial modifications of the standard scheme were necessary. This ultimately results in fairly complicated schemes, inhibiting adoption by engineers. On the other hand, modifications of the conventional finite volume scheme using a Scharfetter-Gummel stabilization towards using dual grids defined via barycenters instead of circumcenters also introduce additional complications for the implementation [6]. Empirical strategies for using the conventional scheme on non-Delaunay grids are also in use, often accepting lower accuracy in exchange for the ability to run any simulations on the available mesh.

II. Cell-Centered Finite Volume Schemes

Modifications of the conventional finite volume scheme proposed by other authors associate the discrete unknowns with the vertices of the mesh. In contrast, we propose to associate unknowns with mesh cells rather than vertices. Since cells are volume elements and material interfaces for typical semiconductor device simulations are commonly aligned at cell boundaries, the proposed cell-centered scheme does not require any additional care at material boundaries, cf. Fig. 1(b).

We follow the usual finite volume discretization procedure for the derivation of a discretization scheme [7]: For a partial differential equation of the form

$$\nabla \cdot \mathbf{F} = g$$

with flux term $\mathbf{F} = \mathbf{F}(u, \nabla u)$ for the unknown function u and volume term $g = g(u)$ which does not depend on any derivatives of u, the first step is to integrate over each cell. Then, the volume integral involving the divergence term is transformed to a boundary integral by means of integration by parts:

$$\int_T \nabla \cdot \mathbf{F} \,\mathrm{d}x = \int_{\partial T} \langle \mathbf{F}, \mathbf{n} \rangle \,\mathrm{d}A$$

for a cell T with outer normal vector $\mathbf{n}$. The crucial ingredient for the derivation of a numerical scheme is the approximation of the fluxes through the cell's facets. To properly account for the conservation property of the underlying partial differential equation, the numerical flux from cell i to cell j needs to be the negative of the numerical flux from cell j to cell i. We propose the following expression for the numerical flux: Consider the connection between the barycenters of the cells i and j. Unlike for dual cells from a Voronoi grid, the connection line $\mathbf{d}_{i,j}$ between the two barycenters is not perpendicular to the respective interface facet $A_{i,j}$ in general, cf. Fig. 1(c). Consequently, additional attention is required for the normal derivative of the numerical flux. For a typical approximation of a constant numerical flux F_h of the true flux $\mathbf{F}$ through the interface, the interface contribution for the flux through the interface $A_{i,j}$ is then computed as for the traditional Voronoi-based method as

$$\int_{A_{i,j}} \langle \mathbf{F}, \mathbf{n}_{i,j} \rangle \,\mathrm{d}A \approx \underbrace{|A_{i,j}| \langle \mathbf{n}_{i,j}, \mathbf{d}_{i,j} \rangle}_{A_{i,j}^{\mathrm{eff}}} F_\mathrm{h} \ ,$$

where $|A_{i,j}|$ denotes the facet volume, $\mathbf{n}_{i,j}$ is the outward pointing unit normal vector on facet j for cell i, and the angle brackets denote the dot product.

978-1-4799-5288-5/14/$31.00

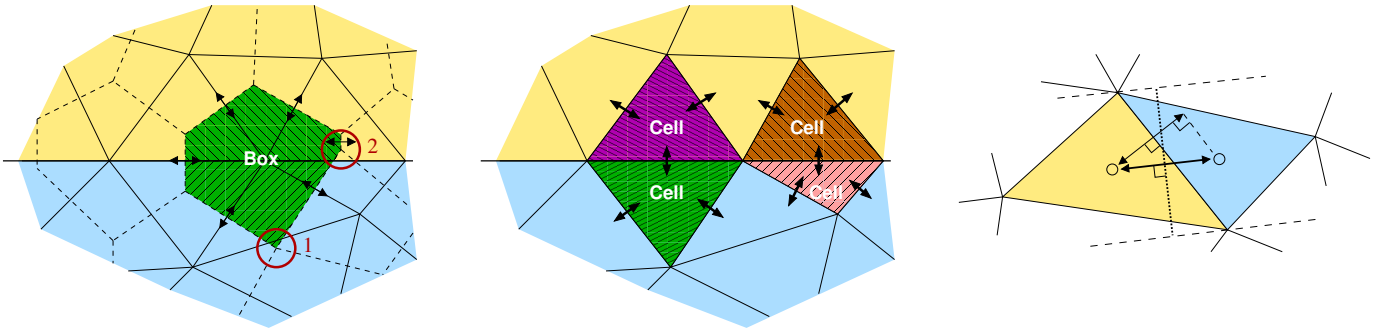

(a) Vertex-based finite volume scheme using Voronoi boxes.

(b) Cell-centered finite volume scheme.

(c) Schematic of the flux reconstruction for the proposed cell-centered scheme.

Fig. 1. A Voronoi box in a vertex-centered finite volume scheme as depicted in (a) may overlap cells not adjacent to the respective vertex (1) or the interfaces of Voronoi cells may not intersect the edge connecting the two vertices (2), which is particularly challenging at material interfaces and in three spatial dimensions. For the typical case of material interfaces resolved by the mesh, such problems do not show up in a cell-centered scheme as in (b) (four cells colored for illustration purposes). We propose to reconstruct the flux between cells based on the values at the barycenters followed by a projection of the non-perpendicular flux onto the facet normal as outlined in (c).

With the barycenter connections $\mathbf{d}_{i,j}$ and the interface contributions $A_{i,j}^{\text{eff}}$ available, only the numerical flux contribution F_{h} needs to be determined. If $\mathbf{F} \equiv \varepsilon \nabla u$ with piecewise constant parameter ε, as is the case for the Poisson equation, F_{h} is simply the difference of u at the two barycenters divided by the distance $\|\mathbf{d}_{i,j}\|$ and multiplied by the harmonic mean of ε at the two barycenters. The harmonic mean ensures that jumps in the permittivity ε at material boundaries are correctly reflected by the numerical solution through corresponding kinks (which translate to jumps of the electric field at material interfaces). If $\mathbf{F} \equiv a\nabla u + \mathbf{b}u$, as is the case for the carrier continuity equations, a Scharfetter-Gummel-like expression for the numerical flux value F_{h} is computed exactly as for the traditional Voronoi-based method by analytically solving the ordinary differential equation obtained from projecting the partial differential equation to the connecting line of the two barycenters. Similarly, expressions for additional equations in the energy-transport or the hydrodynamic model can be obtained.

We note that for the case of structured grids (lines, rectangles, and bricks in one, two, and three spatial dimensions, respectively), the proposed scheme naturally reduces to the traditional Voronoi-based scheme except for the association of unknowns with the cell barycenters rather than vertices. At the same time, the proposed scheme is applicable to general distorted quadrilateral and triangular meshes as well as general hexahedral and quadrilateral meshes for two- and three-dimensional device simulations without requiring a Delaunay property.

III. Results

To demonstrate convergence of the proposed scheme, the numerical solution of the Laplace equation $\Delta\psi = 0$ on the unit square $[0,1]^2$ is compared with the analytical solution $\psi(x,y) = x$, where the respective Dirichlet boundary conditions are prescribed at $x = 0$ and $x = 1$ and homogeneous Neumann boundary conditions are used elsewhere. Unlike typical spline-based approximations of at least first order in finite element methods, the proposed finite volume scheme (as well as the conventional scheme) approximates the analytical solution ψ through a piecewise constant function ψ_{h}, thus the analytical solution cannot be exactly represented by ψ_{h}. The approximation error

$$\|\psi - \psi_{\text{h}}\|_2 = \sqrt{\int_0^1 \int_0^1 (\psi - \psi_{\text{h}})^2 \, \mathrm{d}x\mathrm{d}y}$$

is plotted in Fig. 2 and shows linear convergence with the mesh size parameter h (e.g. the maximum edge length of each triangle) used for generating the different unstructured triangular meshes of the unit square using Netgen [8].

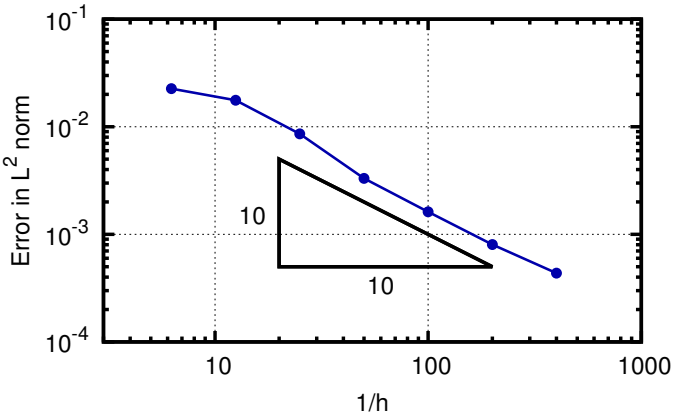

Fig. 2. Plot of the error $\|\psi - \psi_{\text{h}}\|_2$ obtained from a solution of the Laplace equation on the unit sphere with zero Dirichlet boundary conditions at one edge and unit Dirichlet boundary conditions at the opposite edge.

Next we investigate a full randomization of the sidewall of a FinFET with 20 nm channel length using the drift-diffusion model in order to demonstrate the higher flexibility of the proposed cell-centered scheme over the conventional vertex-centered scheme. Homogeneous sidewall roughness of the fin along the transport direction was considered recently in [9], whereas we consider a full, fine-grained randomization of each mesh vertex in the fin. Unlike for the homogeneous sidewall roughness case, the traditional scheme is no longer directly applicable to this more general scenario, because dual Voronoi grids do not exist for general hexahedral meshes.

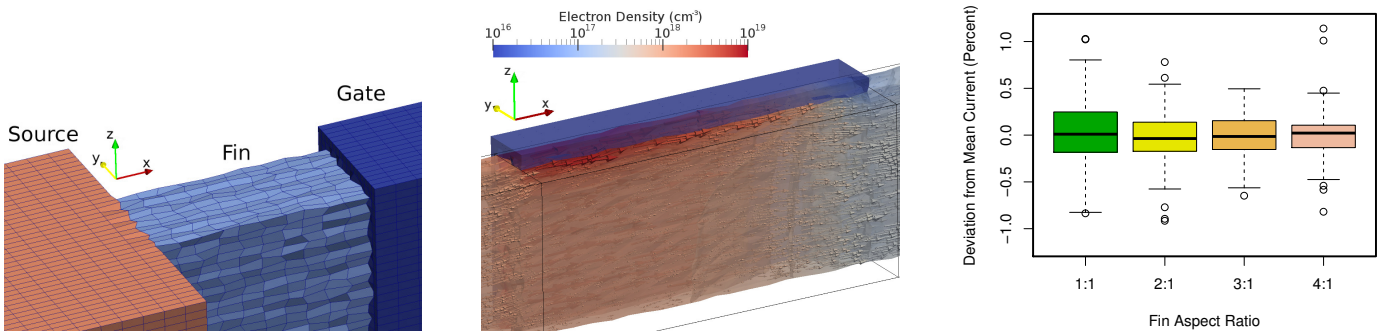

(a) Exemplary mesh after the randomization of vertex locations along a fin (aspect ratio 2:1).

(b) Electron density along the fin which is slit at the center xz-plane. The current flow with arrows is dominant right below the gate oxide.

(c) Evaluation of the relative fluctuations in the drain current for different aspect ratios.

Fig. 3. Geometric surface roughness along the fin of a FinFET with 20 nm channel length using the proposed cell-centered scheme for the drift-diffusion model. The boxplot of simulation results from 100 runs for each of the different aspect ratios (fixed fin height of 9 nm and total length of 40 nm) in (c) suggests that the influence of such a fine-grained geometric roughness only has a small effect, since the resulting fluctuations in the drain current are within about one percent.

We start with a grid of the FinFET consisting of regular bricks with a grid spacing of 1 nm, a fixed fin height of 9 nm, and a total length of 40 nm. Such a grid can be easily set up manually without relying on external mesh generators. Each vertex along the fin is then randomly displaced by $\pm 40\%$ (translating to random displacements of up to ± 0.4nm) of the regular grid spacing. By repeating this procedure, we generated 100 meshes from the underlying regular grid. In addition, fin aspect ratios of 1:1, 2:1, 3:1, and 4:1 are considered in our comparison in order to evaluate the influence of sidewall roughness for different aspect ratios.

The resulting meshes, of which one is depicted in Fig. 3(a), are then simulated using the proposed cell-centered scheme. A sample simulation result depicting the electron density and current flow in the channel along the plane of symmetry of the original undistorted mesh is shown in Fig. 3(b). The boxplot of simulation results from 100 runs for each of the different aspect ratios (fixed fin height of 9 nm and total length of 40 nm) in Fig. 3(c) suggests that the influence of such a fine-grained geometric roughness only has a small effect: For the considered drain bias of 1 Volt and a gate bias of 0.8 Volt the resulting fluctuations in the drain current are within about one percent. Furthermore, no significant change in the variance of the currents is observed across the different fin aspect ratios. We explain this by the fact that the main current flow is located right below the gate oxide, hence the fin aspect ratio only affects the mean current, but does not have a significant influence on the variance.

It should be noted, however, that our study of fin sidewall roughness does not include the consideration of quantum-mechanical effects, through which the current flow attains its maximum away from the oxide interface. In such case, quantum corrections or even full solutions of the Schrödinger equation should be conducted to better capture these geometric effects. Regardless, we conclude that random high-frequency fluctuations in the fin sidewall roughness do not show a significant influence on the current. Instead, attention for future investigations should be on systematic variations such as those induced by processing steps, which are typically of low frequency and higher spatial correlation.

Finally, we consider the simulation of a simplified n-channel laterally diffused metal oxide semiconductor (LDMOS) device on an unstructured, spatially triangular grid of 18 Volt and a gate voltage of 2 Volt. We apply the proposed cell-centered scheme to the spatial domain of the spherical harmonics expansion (SHE) method for obtaining deterministic numerical solutions of the Boltzmann transport equation [10]. Following the state-of the art for the SHE method, the H-transform and a maximum entropy dissipation scheme is employed for stabilization. Full-band effects are considered by using full-band data for the carrier velocity and the density of states [11].

The simulation results depicted in Fig. 4 demonstrate that our scheme is applicable even at a drain-source bias of 18 Volt, which is higher than any bias conditions reported for the SHE method so far. For this purpose several challenges had to be overcome: First, the H-transform implies a linear dependence of the total energy (H) range on the applied bias. To limit the computational effort and memory requirements at high applied bias, the kinetic energy range is limited to 5 eV within the total energy range of 22 eV, cf. Fig. 4(a). The second challenge is to numerically resolve the distribution function over more than 70 orders of magnitude due to the high bias and the resulting high-energy tail of the distribution function. We achieve this through a rescaling of the distribution function by the Maxwellian equilibrium distribution at each point in the device. Still, tight tolerances are required in the preconditioned iterative linear solver in order to prevent premature termination and inaccurate results.

The plot of the average carrier energy in Fig. 4(b) shows that carriers may reach average energies as high as 1.75 eV, which stems from the high bias between gate and drain and the induced acceleration of carriers. While the energy distribution function near the source contact and the gate is close to a Maxwellian, carriers gain energy due to the high electric field along the drain extension. When reaching the drain region, the energy distribution of carriers is nearly flat over a range of 4 eV, cf. Fig. 4(c), demonstrating that the onset of the thermal tail of the distribution function is pushed to very high energies.

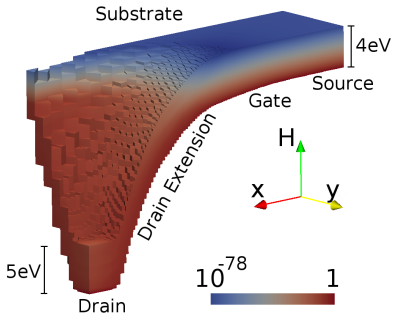

(a) Electron distribution function in (x, y, H)-space. The mesh profile along total energy H resembles the conduction band edge.

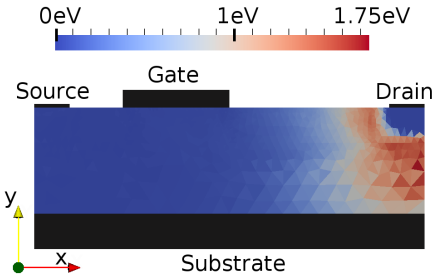

(b) Average carrier energy for each cell.

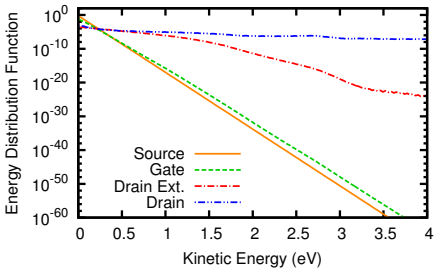

(c) Energy distribution functions at selected points between source and drain.

Fig. 4. Simulation of an n-channel laterally diffused metal oxide semiconductor (LDMOS) device at a source-drain bias of 18 Volt and a gate voltage of 2 Volt using the proposed cell-centered finite volume scheme for computing first-order spherical harmonics expansion solutions of the Boltzmann transport equation without Pauli exclusion principle.

IV. Summary and Conclusion

A cell-centered discretization scheme is proposed which addresses the disadvantages of the traditional Voronoi-based discretization for unstructured grids. It can be used on arbitrary structured and unstructured grids in one, two, and three spatial dimensions and is simpler to implement than the alternatives suggested in the past. In particular, it considerably simplifies the treatment of material interfaces, as the unknowns are associated with cells, which are commonly associated with a certain material, rather than vertices, which may be adjacent to multiple materials. The M-matrix property of the system matrix obtained via the traditional Voronoi-based discretization holds equally true for the proposed cell-centered scheme. This helps to avoid spurious negative values for the numerical approximations of non-negative physical quantities such as carrier densities [12].

We demonstrated the applicability of the proposed scheme by three examples: First, we empirically showed the convergence of the method on an unstructured triangular grid for the Laplace equation on the unit square. A rigorous analytical proof, however, is left to future work. Second, we applied the scheme for studying microscopic variations of the sidewall roughness of a FinFET through random displacements of the underlying regular grid. A similar study using the traditional Voronoi-based discretization would require a tedious Delaunay mesh generation step and may introduce spurious numerical diffusion, whereas our scheme can be applied directly. Third, we showed that the method is also applicable to the SHE method for obtaining deterministic numerical solutions of the Boltzmann transport equation for an nLDMOS device at a source-drain bias of 18 Volts. We expect this to allow for new insights in the modeling of hot carrier degradation, cf. e.g. [13], as the distribution function is available over energies of several electron Volts and over many orders of magnitude free from stochastic noise.

A reference implementation of the proposed scheme for the drift-diffusion model as well as the spherical harmonics expansion method for the Boltzmann transport equation is available in the free open source simulator ViennaSHE [14].

Acknowledgment

This work has been supported by the Austrian Science Fund (FWF), grant P23598.

References

[1] S. Selberherr, *Analysis and Simulation of Semiconductor Devices*. Springer, 1984.

[2] S.-W. Cheng, T. K. Dey, and J. Shewchuk, *Delaunay Mesh Generation*. Chapman and Hall/CRC, 2012.

[3] J. J. H. Miller, W. H. A. Schilders, and S. Wang, "Application of Finite Element Methods to the Simulation of Semiconductor Devices," *Reports on Progress in Physics*, vol. 62, no. 3, p. 277, 1999.

[4] D. J. Cummings, M. E. Law, S. Cea, and T. Linton, "Comparison of Discretization Methods for Device Simulation," in *Proceedings of SISPAD*, 2009, pp. 1–4.

[5] P. Bochev, K. Peterson, and X. Gao, "A New Control Volume Finite Element Method for the Stable and Accurate Solution of the Drift-Diffusion Equations on General Unstructured Grids," *Computer Methods in Applied Mechanics and Engineering*, vol. 254, pp. 126 – 145, 2013.

[6] M. B. Patil, "New Discretization Scheme for Two-Dimensional Semiconductor Device Simulation on Triangular Grid," *IEEE Transactions on Computer-Aided Design of Integrated Circuits and Systems*, vol. 17, no. 11, pp. 1160–1165, 1998.

[7] J. Bey, *Finite-Volumen- und Mehrgitter-Verfahren für elliptische Randwertprobleme*. B. G. Teubner, 1998.

[8] "Netgen," http://sourceforge.net/projects/netgen-mesher/.

[9] N. Agrawal, Y. Kimura, R. Arghavani, and S. Datta, "Impact of Transistor Architecture (Bulk Planar, Trigate on Bulk, Ultrathin-Body Planar SOI) and Material (Silicon or III-V Semiconductor) on Variation for Logic and SRAM Applications," *IEEE Transactions on Electron Devices*, vol. 60, no. 10, pp. 3298–3304, 2013.

[10] S.-M. Hong, A.-T. Pham, and C. Jungemann, *Deterministic Solvers for the Boltzmann Transport Equation*. Springer, 2011.

[11] S. Jin, S.-M. Hong, and C. Jungemann, "An Efficient Approach to Include Full-Band Effects in Deterministic Boltzmann Equation Solver Based on High-Order Spherical Harmonics Expansion," *IEEE Transactions on Electron Devices*, vol. 58, no. 5, pp. 1287 –1294, 2011.

[12] A. Bermann and R. J. Plemmons, *Nonnegative Matrices in the Mathematical Sciences*. Society for Industrial and Applied Mathematics, 1987.

[13] S. E. Rauch and G. La Rosa, "The Energy-Driven Paradigm of NMOSFET Hot-Carrier Effects," *IEEE Transactions on Device and Materials Reliability*, vol. 5, no. 4, pp. 701–705, 2005.

[14] "ViennaSHE," http://viennashe.sourceforge.net/.